Nanoscale Adsorbed Water Layer and Macroscopic Soil Properties

Wes W. Wallender*[1], Don P. Land[2]

Project Objectives Addressed

1. Use atomic force microscopy (AFM) to measure thickness of the adsorbed water layer in montmorillonite clay platelets as affected by the electrochemical properties of the water.
2. Incorporate the pertinent adsorbed water properties into an appropriately modified Kozeny-Carman equation.
3. Use the modified Kozeny-Carman equation with adsorbed water properties to predict effective porosity and saturated hydraulic conductivity for clay.

Approach and Procedures

Macroscopic soil properties such as hydraulic conductivity, water retention and porosity are critical variables in the evaluation of flow and transport processes in soil systems, which, in turn, are critical components of modeling toxics dispersion, nutrient retention, restoration, remediation, hydrologic engineering projects, and effects of agricultural and urban development, among others. The presence and properties of adsorbed water around clay and its affects on the effective porosity and hydraulic conductivity of the soil matrix have been investigated by various researchers since the early 1970s.[1] According to these and many subsequent authors, the water in the soil pores is said to be distributed between two phases. Phase 'a' containing the so-called free water, which is free to flow under a hydraulic gradient, and phase 'b', which is directly affected by the particle surface forces.[2] The phase 'a' water essentially behaves as a Newtonian fluid, while the phase 'b' water, when highly confined in the interlamellar spaces between clay platelets, is reported to show an increase in effective viscosity and an elastic behavior, indicative of a solid-like structure rather than that of a fluid.[3,4] The thickness of this solid-like water layer is not fixed but is a function of the electrochemical environment.[5] The adsorbed water bound to the mineral particle is immobile and reduces the effective pore volume of the soil system and thus the fraction of total pore space available for flow, i.e. the effective porosity. Some recent results using nuclear magnetic resonance relaxation suggest, however, that the interlamellar water layer is nearly as mobile as the "free" water in the bulk solution.[6-10] Despite the widespread acceptance of the role of adsorbed water layer in affecting hydraulic conductivity, water retention, and porosity, none of the available prediction methods for these hydraulic parameters account for the effects of the adsorbed water layer on these properties.[11] This is primarily because it is difficult to measure and quantify the properties of the adsorbed water layer and it disposition and so neither the properties of the adsorbed water as a function of the electrochemical properties of the water, nor its effects on the process, are reported in the literature. Thus, the understanding of the properties of the adsorbed water layer in clay minerals

[1] Departments of Land, Air and Water Resources and Biological and Agricultural Engineering, UC Davis

[2] Department of Chemistry, UC Davis

*Principal Investigator

For more information contact Dr. Wesley Wallender (wwwallender@ucdavis.edu)

as a function of electrochemical properties of the water and its affect on hydraulic properties of a soil system is a crucial challenge, as well as an opportunity.

The aim of this project is to use the unique capabilities of atomic force microscopy (AFM – also known as scanning force microscopy - SFM) to study small tactoids of clay platelets in aqueous environments and attempt to measure the confined absorbed water layer between the clay platelets. Sodium montmorillonite (MMT) clay is a 2:1 layered aluminosilicate from the smectite group with the Unit Cell formula $Na_{0.66}(OH_4)Si_8(Al_{3.34}Mg_{0.66})O_{20}$. The Al and Mg atoms are located in the octahedral sites coordinated to oxygen atoms and hydroxyl groups forming the central octahedral layer of each clay sheet. Silicon atoms in tetrahedral sites are coordinated to the oxygen atoms and form two layers on either side of the octahedral layer. The overall configuration of a single clay platelet is a tetrahedral-octahedral-tetrahedral "sandwich". The sheets have a permanent negative charge resulting from isomorphic substitutions occurring mainly in the octahedral layer. The charge is balanced by sodium ions intercalated between the sheets.[5,12]

In 1994, Dove and Chermak predicted that the measurement of differences in vertical heights to within few hundredths of a nanometer would prove useful in understanding the effects on clay particles brought about by changes in the chemical environment.[13] However, to the best knowledge of the authors, the use of scanning probe microscopy (SPM) for the sub-nanometer measurements of interlayer spacing of clays has not yet been reported. Herein are the first such results. In addition, the use of non-contact (tapping) mode force microscopy allows the simultaneous acquisition of phase data. Since the surfaces contacted by the AFM tips are chemically identical, phase differences can be directly attributed to the relative surface elasticity. Thus, stacks of two hydrated clay platelets are shown to have a lower Young's modulus that a single hydrated clay platelet and both have Young's moduli smaller than that of the mica surface.

Methods

AFM uses a sharp tip on the end of a flexible cantilever rastered over the surface in question. Forces between the tip and the surface cause a deflection in the cantilever. The deflection is amplified by a laser beam reflecting off of the cantilever and striking a position sensitive photodiode array. Ultimately, one obtains a high-resolution topographic image of the surface with typical resolution of ~0.01 nm in the vertical dimension and ~0.5 nm in the horizontal dimensions. For imaging clay platelets in contact mode, one must use minimum applied normal force to avoid damaging the surface or moving platelets (Eggleston, 1994). This allows one to develop a map of useful topographical features, such as single, isolated platelets and stacks of two or more platelets.

Contact mode imaging works well for dry samples. However, for samples immersed in water, direct contact mode always leads to tip-induced changes in the adsorbed clay platelets. However, immersed samples were found to be resilient under non-contact (tapping) mode imaging. In this mode, the tip/cantilever system is induced to vibrate near its resonant frequency by driven oscillations in the z-piezo (which controls the height of the tip). The tip oscillation amplitude and relative phase are both monitored simultaneously during scanning. Interactions with the surface can affect either the amplitude or the phase or both. When the tip, near the bottom extremum of its travel, encounters the surface, the amplitude decreases. Feedback circuitry activates the z-piezo to adjust the height until the set amplitude is re-established. In this way, a relatively constant tip height is maintained during scanning. The image is formed by

plotting the z-piezo position (voltage) as a function of (x,y) coordinate across the image. This is a so-called topography, or height image.

The relative phase between the tip and the driving force is also monitored as a function of (x,y) coordinate. This is called a phase image. In a constant amplitude experiment, changes in the phase of the tip oscillation can be interpreted as changes in the chemical or mechanical forces encountered when the tip and sample interact. In general, attractive forces between the two cause the tip phase to lag more, while repulsive forces reduce the phase lag. Similarly, softer surfaces would increase the phase lag and harder surfaces would reduce it. Many other types of interactions may affect the relative phase, such as changes in chemical composition of the surface or near-surface region, changes in magnetism (if the tip has magnetic properties), etc. For the experiments described here, using MMT platelets deposited on mica in water, there are only two types of surface encountered by the tip: mica and MMT.

The following experiments are performed on an Asylum Research MFP-3D Atomic Force Microscope. Tapping mode images are made with Asylum Research TR800PSA triangular cantilevers with silicon nitride tips. Typical scan speeds are 1 Hz. In tapping mode, the resonant frequency is about 20 kHz, with small variations from cantilever to cantilever. Sodium montmorillonite clay is used as delivered from Gelest, Inc. Type I ultra pure water is purified using a Millipore Synergy UV filtration system. Mica sheets were purchased from Ted Pella. Sonication was done using an L&R Ultrasonics, model Quantrex 210, 335W 43 kHz sonicator.

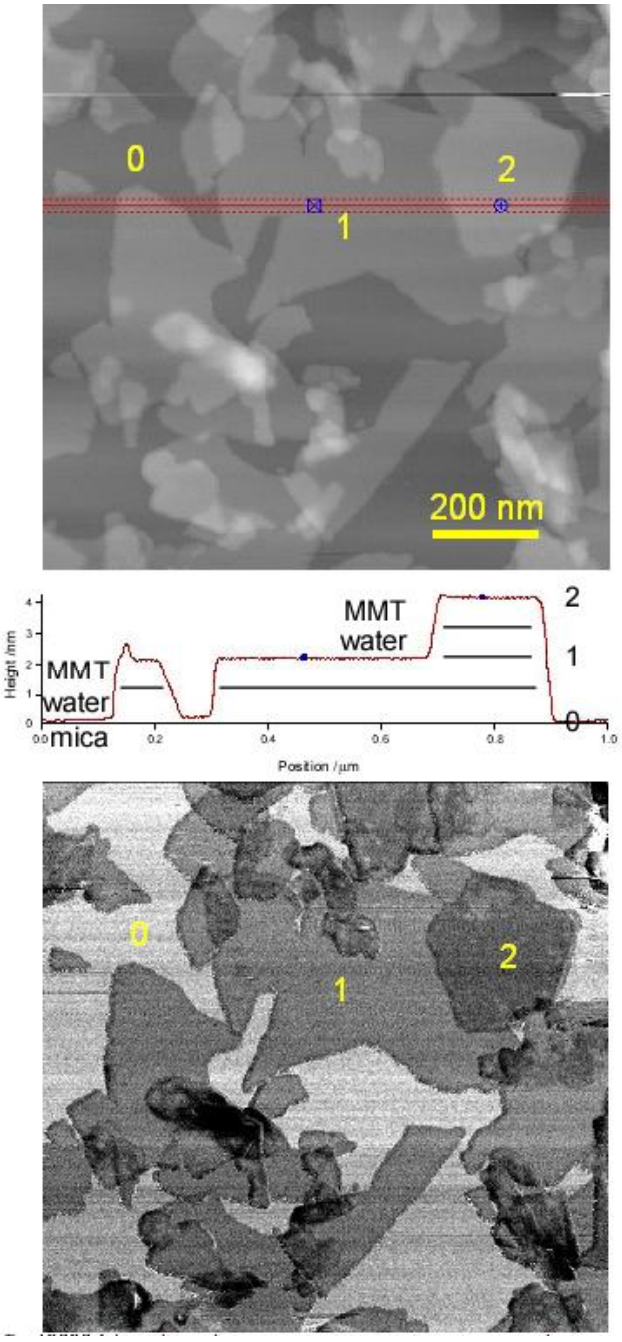
To verify the accuracy and calibration of the vertical resolution of the AFM, the instrument was standardized using a (111) gold surface that was annealed with H_2 flame prior to scanning. A monoatomic gold step-height of 0.24 nm[14] was used as a standard calibration and the microscope showed excellent agreement with the literature value.

When clay is placed in water and agitated, water enters the interlamellar space of the clay stacks and expands the clay tactoids until the individual nanoplatelets become completely separated. In order to study the clay nanoplatelets with the Atomic Force Microscope (AFM), it is first necessary to fully exfoliate the clay tactoids, followed by deposition on a suitable surface. The mica surface is chosen because it provides an atomically smooth surface with very few impurities. The individual clay nanoplatelets are prepared in the following manner. First, about 2 milligrams of Sodium montmorillonite clay powder is placed in 100 mL of Type I pure water. The clays are exfoliated in an ultrasonic bath for 8-12 hours. After this, the resulting suspension is allowed to settle. If kept clean, the solution is very stable and the fully exfoliated individual clay sheets will stay in suspension for many months. Several drops of the suspension are then placed on a clean, freshly cleaved mica disk, roughly 1mm in diameter; the solution is then allowed to stand for a few minutes. The excess water is then removed by heating the sample on the hot plate for several minutes until all the water has evaporated, this will insure that all of the clay nanoplatelets have a chance to orient and adhere to the mica surface. After the sample is cooled several, drops of ultra pure Type I water are deposited onto the prepared sample in order to fully hydrate the clay tactoids. Scanning is then preformed in this solution. The clay nanoplatelet coverage on a surface can be controlled by adjusting the amount of clay solution that is deposited onto the substrate.

Results

Imaging Surface Topography and Elasticity

An example of a tapping mode image of MMT platelets on mica in water is shown in Figure 1 (top image), which shows a 1 μm by 1 μm AFM amplitude (height) mode topographic image. For this image, darker shades of gray indicate smaller values of the height. The lowest terraces in this image are the mica surface (labeled 0), which is observed to be atomically smooth with very few impurities. Average terrace widths of the mica surface with no clay particles are several mm wide, so the higher terraces observed here are several MMT particles. In many regions, one observes stacks of two and three and maybe more clay platelets.



The horizontal red line in the height image represents a single scan line across the image. The height values along this line are presented in the plot just below the image. The height data are plotted in red (512 data points). Again, the lowest level (0) is mica. Moving up, the next terraces represent a single MMT clay platelet. Since these images are obtained in water, the clay is fully hydrated, yielding a total height (platelet, ~ 1 nm, plus water, ~ 1 nm) of about 2 nm.

Figure 1

On the right side of the image, the red line cuts across a region with a second clay platelet on top. The height trace goes up to ~ 4 nm above mica, from the addition of a second hydrated MMT platelet. This is indicated by the solid horizontal black lines and the labels on the left side of the plot.

The bottom image in Figure 1 is a phase image obtained at the same time as the height image. In the phase image, darker regions represent larger phase lag. The mica substrate has the least phase lag, while the MMT regions show greater phase lag. In fact, taller stacks of MMT platelets show even greater phase lag.

While mica and MMT have very similar composition, there are clearly significant differences. After all, mica and MMT take on significantly different macroscopic forms. One can argue that the majority of the differences are governed by the lateral extent of individual platelets. Mica, with relatively few impurities and, thus, long range crystallographic coherence, forms platelets that can extend mm, cm, and even longer. Each mica sheet is almost exactly like the next, so when they stack, there is high commensurability, since there are few defects. In MMT, however, the presence of numerous defects from metal ion substitutions means that individual platelets grow to be, at most, a few µm. Thus, MMT tactoids are typically no larger than a few µm in any dimension. In addition, those impurities also lead to a significant residual negative charge on the individual platelets, which leads to the presence of counter ions at the interface.[15] The presence of the counter ions and the lack of long-range crystal coherence both contribute to the ease with which water intercalates into the interlamellar spaces in MMT, while mica shows no such propensity to swell in water. Thus, there are at least two possible explanations for the differences in the phase shift of mica and MMT: (1) changes in the tip-surface interactions due to differences in the surface charge and composition of the two types of surface; and/or (2) changes in the tip-surface interactions due to differences in the elasticity of the two types of surface. It is impossible to tell the relative importance of these two contributions to the phase shifts without very sophisticated and difficult experiments. However, the surface charge and surface composition of small regions of mica and MMT are very similar, and it is likely that the differences observed here are from differences in elasticity, since the mica regions have no intercalated water.

If one considers the origins of the phase shifts between different MMT regions, however, the analysis becomes much more definitive. Note that the phase shift observed is very constant over any single MMT platelet and is also very constant from one particle to another, so long as they occupy the same level in a stack (determined by reference to the height image). That is, all single platelet MMT particle stacks have the same phase shift value, as do all of the two particle stacks, etc. This is likely due to very similar elasticity, chemical composition and surface charge for all platelets at the same level. Thus, the changes observed from one MMT level to the next are likely to arise solely because of differences in the elasticity. That being the case, one can deduce that taller stacks of hydrated MMT platelets appear to have smaller Young's moduli than do shorter stacks. This is, perhaps, not surprising. Individual MMT platelets are known to be very compliant. One can observe the degree of compliance by observation of the regions where one platelet overlaps with another. The transition is essentially instantaneous, with barely any perceptible slope in the transition region, as imaged here. The intercalated water layer between compliant platelets contributes to the low level of elasticity.

Quantitative Measurement of Interlayer Spacing: Intercalated Water

One of the goals of this project is the quantitative measurement of interlayer thickness as a function of chemical environment. The aluminosilicate platelet of MMT is a stable structure with a thickness of 0.955 nm. However, water intercalates into the interlamellar space, causing the platelets to separate – MMT clay swells when wet. The equilibrium separation results from a balance between attractive forces (between the negatively charged platelets and the positively charged counter ions) and repulsive forces (pressure due to intercalated waters of solvation). We propose to measure the platelet separation to infer properties of the intercalated water and its environment. One might expect changes in pH, ionic strength, or the nature of the counter ions to have an effect on the equilibrium platelet separation. A baseline for these types of measurements is achieved by measuring the platelet stacks while immersed in pure water. However, platelets immersed in water can move under influence of the AFM tip when imaging in direct contact mode. Thus, non-contact, or tapping mode is used to image immersed platelet stacks.

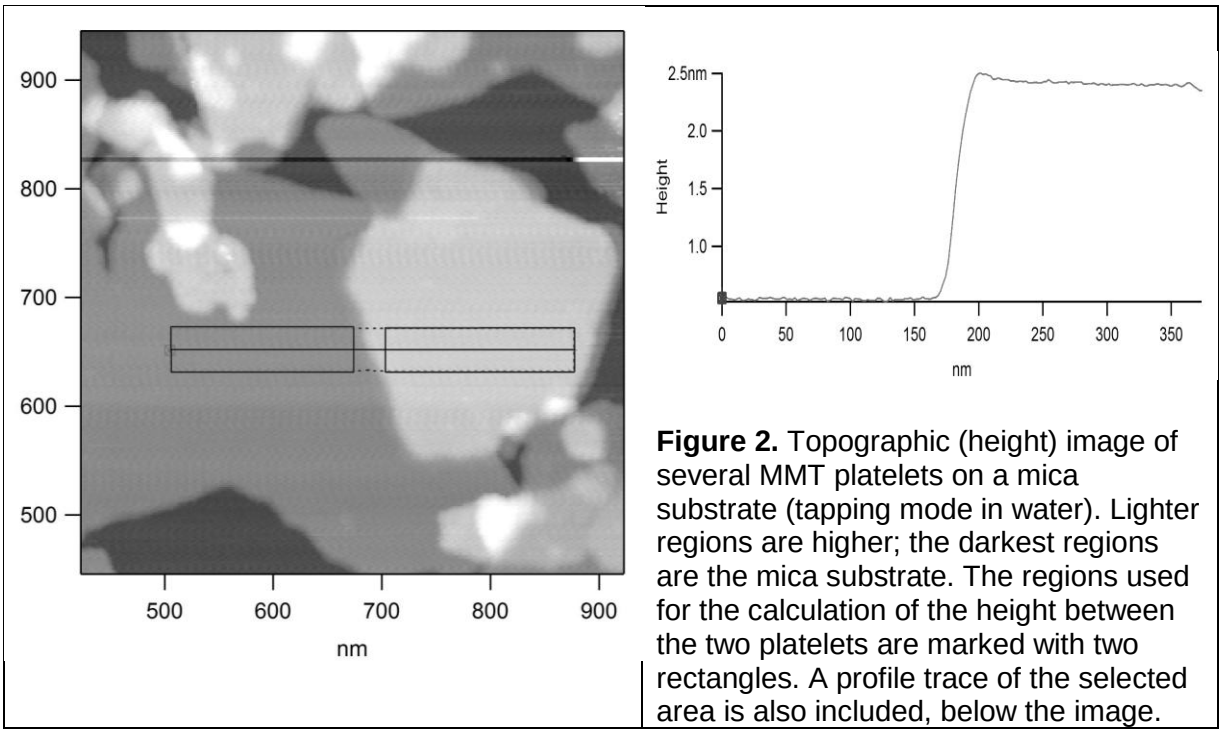


Figure 2. Topographic (height) image of several MMT platelets on a mica substrate (tapping mode in water). Lighter regions are higher; the darkest regions are the mica substrate. The regions used for the calculation of the height between the two platelets are marked with two rectangles. A profile trace of the selected area is also included, below the image.

In order to measure the separation distance between the clay nanoplatelets, areas are selected that are relatively free of noise and show a good overlap of at least two clay nanoplatelets. Figure 2 shows one such selection. An area on the lower platelet is selected to define a reference plane. The rest of the image is flattened with respect to that plane. This removes most of the residual slope from the region around this reference. Next, approximately equal numbers of data points are selected on the top and bottom clay platelets near the reference region. In order to determine the height separation between the two regions, all of the points from the lower area are averaged and subtracted from the average of all of the points in the higher area. Note that the region near the step is excluded to avoid including transitional data points. A typical single height measurement is based on approximately three thousand data points (1500 for each level), giving a good statistical representation. Figure 3 shows a histogram of the ~3000 height values in the two regions (including the step region) from which the separation distance was calculated.

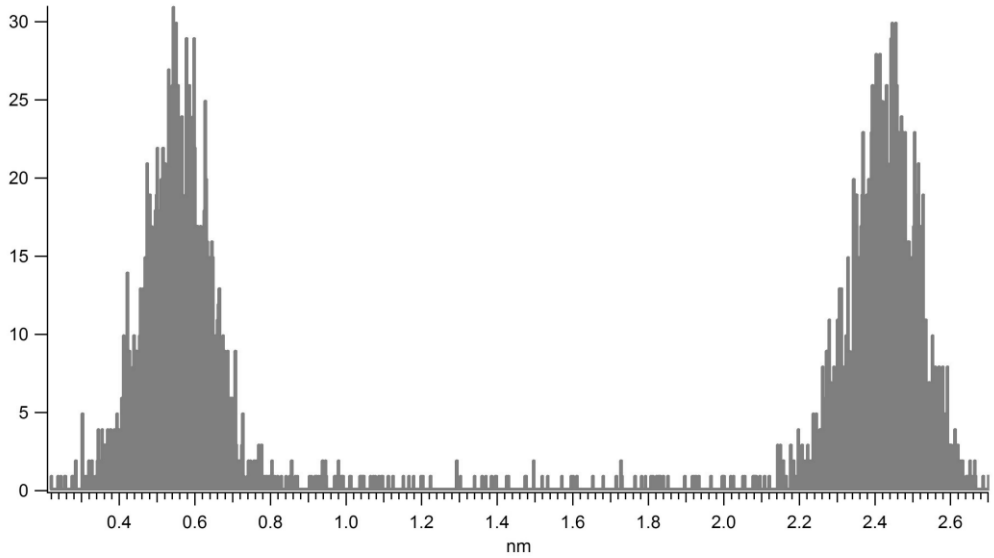


Figure 3. A histogram plot of the ~3,000 height data in the two regions marked in Figure 2. Data between the two regions is also included in the histogram plot, and appears as the low-level of intermediate values representing the transition. This transition region is not included in the separation distance calculations.

After making close to 120 measurements and being careful to select only the best sites for our measurements, our experiments showed an average separation between two fully saturated (submerged) clay nanoplatelets within a tactoid of 1.82 nm, with a standard deviation of 0.21 nm and 95% confidence limit of ±0.04 nm. A Histogram distribution of our measurements is displayed in Figure 4 showing a good Gaussian distribution around the average value.

With an average thickness of a single water layer of 0.25 nm[16] and a fundamental crystallographic thickness of a single clay nanoplatelet of 0.96 nm[5] our experiment would suggest that in a fully saturated (submerged) Sodium montmorillonite clay tactoid, two parallel clay platelet are separated by approximately 3 layers of water confined in the interlamellar spaces. Our findings are in good agreement with Cases and coworkers[17] who were able to make measurements using controlled-transformation-rate thermal analysis, nitrogen adsorption volumetry, and x-ray diffraction, to estimate the total layer height and the number of layers of

adsorbed water between platelets, and the average number of platelets per tactoid for montmorillonite clays under various conditions of hydration. The degree of hydration was controlled by treating dried samples with exposure to air at different relative humidities. For oven-dried tactoids, the total layer height is reported to be 0.955 nm. After hydrating in a low relative humidity environment for an extended period of time, the tactoid platelets were estimated to contain one layer of water of hydration and the total layer height was estimated to have expanded to 1.249 nm.

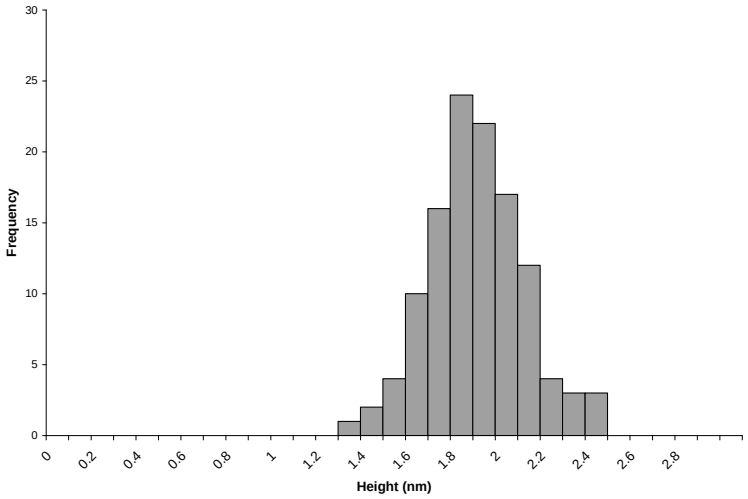


Figure 4. A histogram plot of the ~120 height difference measurements between two Sodium montmorillonite clay platelets in water, each derived from the average of thousands of individual height measurements (image pixels). Average = 1.82 nm, with a standard deviation of 0.21 nm and 95% confidence limit of ±0.04nm.

Hydration to the level of two layers of intercalating water resulted in an estimate of 1.555 nm and full hydration lead to estimates of three layers water and a total layer height of 1.81 nm[17]. Thus, our measurement of 1.82 ± 0.04 (95% confidence limits) is in excellent agreement with their estimate of that for a fully hydrated tactoid with three layers of water separating neighboring platelets.

Effect of Salinity on the Thickness of the Interlamellar Water Layer of Na MMT

The above results show that we are able to accurately measure the thickness of the interlamellar water layer. The next objective was to observe whether changes in the chemical environment would affect the inter-platelet separation distance. A set of experiments were carried out to investigate the relationship between immersed platelet separation distance and salinity. In these experiments, NaCl was added to the suspension of exfoliated clay particles at varying concentrations. Next, mica surfaces were exposed to the solutions as before and dried. The volume of solution deposited was accurately monitored. After drying to adhere the platelets to

the mica, the samples were rehydrated with pure water, as before, but using the exact same volume as was present before drying. Since the NaCl present in the original solution was still present after drying, the solution for scanning should have the same concentration of NaCl as that used in the preparation. The pink triangle data point was obtained by adhering the platelets to a mica surface using pure water, then rehydrating with 0.15 M NaCl solution (Figure 5). No significant difference was observed.

Figure 5 shows a plot of the inter-platelet separation measured as a function of NaCl concentration from 0.0 to 0.3 M. No significant change is observed. This result indicates that, for the range of salinity investigated, concentration of NaCl plays little role in establishing the equilibrium platelet spacing. It is reasonably well accepted that water in the interlamellar space is ordered into individual layers. Spacings of 0, 1, 2, or 3 layers are observed, but intermediate, non-integer values are not.[4,17] Several theoretical studies have also come to this conclusion.[18-21] That being the case, the interlamellar spacing is dominated by water-water interactions. The interlamellar space of Na-MMT already consists of Na counter ions that get solvated by the water. The concentration of Na^+ in this space is determined primarily by the surface charge of the platelets, and the presence of NaCl in the bulk solution plays little role in determining the chemistry in the interlamellar space.

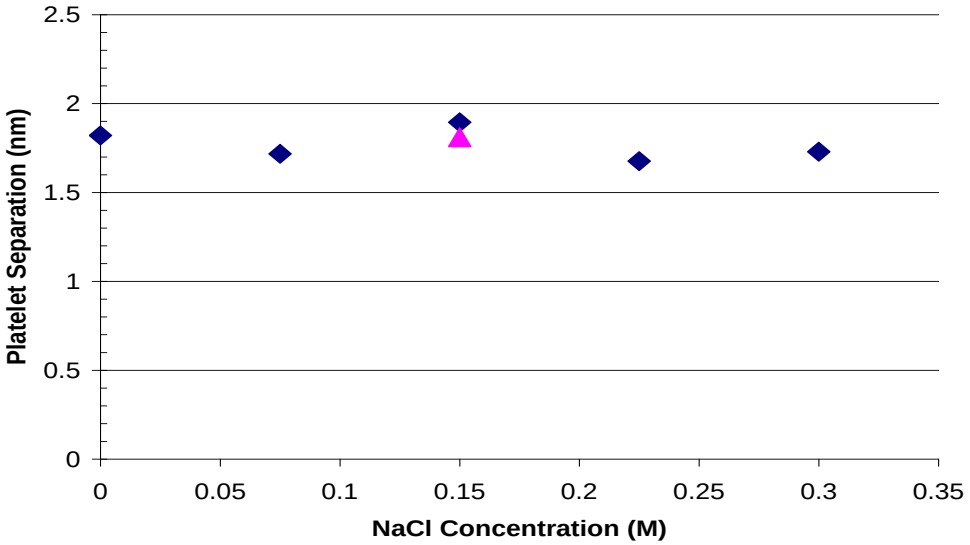


Figure 5: Plot of the average inter-platelet distance as a function of NaCl concentration. Over this range of salinity, there appears to be little effect on the equilibrium separation distance.

Stochastic Channel Formation during Drying of Clay Particles

An example of a stack of two clay platelets in the process of drying is shown in Figure 6. Near the bottom of the imaged stack of two platelets (the large, bright feature that occupies the region from 400 nm to the top in "y" and from 0.95 to 1.3 μm in "x"), it is evident that the loss of water takes place at different rates on different regions of the samples. The low regions of the upper clay platelet are 0.51 nm below the higher regions. This is the expected height of two water

layers. Thus, the low regions have a single layer of water between subsequent platelets, and the higher regions are still in the fully saturated state, with three layers of water. Theoretical molecular dynamics modeling has indicated that the first layer of water is very tightly bound, but that the second and third layers are bound much less tightly with about the same energy.[22] We are early in the process of modeling the dynamics, but this clearly has implications in the prediction of the swelling and drying behavior of clays. We have observed this phenomenon on 6 different occasions for partially dried samples. It is, as yet, unclear what combination of conditions leads to their presence. In another case, the system of channels and ridges has a height difference of 0.25 nm, or one layer of water. The differences are always an integer multiple of 0.25 nm, or the thickness of one water layer.

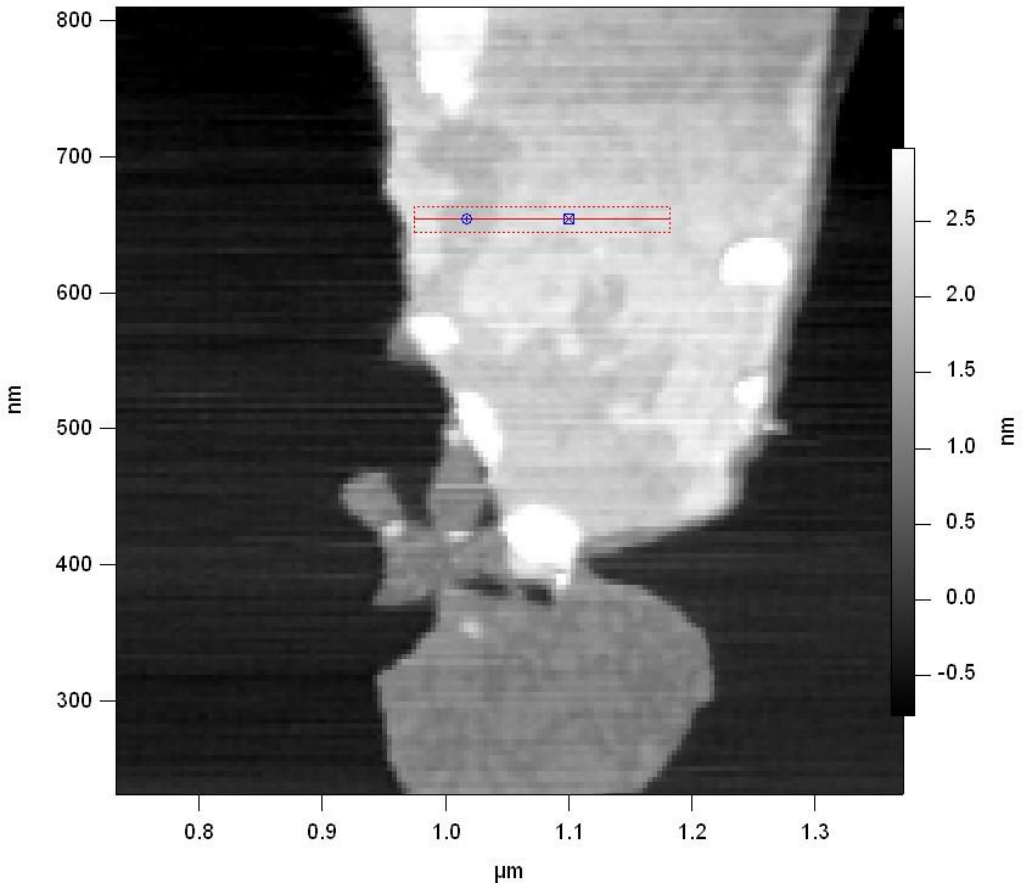


Figure 6: Montmorillonite platelets on a mica surface after partial drying. Height mode: lighter features are higher. The darkest areas are the mica substrate. A stack of two clay platelets is observed extending from the upper edge down about three quarters of the way to the bottom. That this is a stack of two particles can be discerned by observing the extension of the lower platelet, particularly at the right edge, and also by comparison with the single ellipsoidal platelet directly below it. Small brighter regions are a third level of platelets. The upper terraces of the both the single platelet and the stack show a mottled appearance. This is due incomplete loss of two of the three water layers that separated the platelets from the mica surface when fully hydrated. The horizontal line near the top indicates a height trace that yields a difference in the slightly darker and lighter regions to be 0.51 nm – two water layers.

Modified Kozeny-Carman equation

The Kozeny-Carman equation is based on the assumption that flow in the pores of soil can be approximated by flow through an assembly of tubes. The Hagen –Poiseuille law together with Darcy's law yields

$$K = \left(\frac{\Delta L}{\Delta L_e}\right)^2 n\left(\frac{\rho_w g R_h^2}{c\mu_w}\right)$$

in which K is the scalar hydraulic conductivity, ΔL is linear distance of the flow conduit, ΔL_e is the curvilinear length of the capillary path, $(\Delta L/\Delta L_e)^2$ represents the tortuosity τ of the flow conduits, R_h is the hydraulic radius of the flow conduits, and c is a parameter resulting from the conversion of radius of flow capillary to the hydraulic radius. The postdoctoral scholar proposed for this study together with the principal investigator have recently derived a generalized mechanics-based macroscopic saturated hydraulic conductivity equation incorporating the effects of effective porosity, flow geometry and tortuosity as a function of the adsorbed water layer properties.[25] The effective porosity with correction for adsorbed water layer thickness (n_{ad}) is given by,

$$n_{ad} = 1 - C_F(1 - n)$$

in which C_F is porosity correction factor and is a function of adsorbed water layer thickness and mass specific surface area of the soil particle. The modified Kozeny-Carman equation is expressed as

$$K = C_1\left(\frac{g}{\mu_w \rho_w}\right)\frac{n_{ad}^3}{(1-n_{ad})^2 S^2 G_s^2}$$

where parameter C_1 is represented by

$$C_1 = \frac{\tau}{c(1-\chi)^2}$$

with χ being the fraction of the surface area of the soil particles ($0 \le \chi < 1$) not in contact with the flowing water. The parameter χ is related to the inter-particle contact area, which in turn is a function of the inter-particle contact load and the elastic properties of the adsorbed water layer (Singh and Wallender 2007). Thickness of the adsorbed water layer and mass specific surface area of the clay particle is used to derive the porosity correction mode.[25]

The use of adsorbed water thickness adjusted porosity in the modified Kozeny-Carman equation to predict the saturated hydraulic conductivity for clays yields an improved prediction of the saturated hydraulic conductivity.[25]

Discussion

Careful measurements of clay nanoparticles yield a wealth of information. The phenomenon of water intercalation in clay has been studied by others with various methods, which include controlled-rate thermal analysis, nitrogen adsorption volumetry, water adsorption and desorption gravimetry, immersion microcalorimetry in water, and most notably, X-ray diffraction.[17,23] These methods all analyze bulk material, averaging over hundreds of thousands of particles or more.

Such averaging methods have little or no ability to measure such things as individual particle morphology, impurities and anomalies. In addition, little detail is provided on what is the actual distribution of values. With the use of AFM, we are able to easily observe small clay tactoids as well as single clay nanoplatelets and take accurate measurements of clay particles in their most natural environment. Our measurement of 1.82 ± 0.04 nm (95% confidence limits) is in excellent agreement with other estimates[17] for a fully hydrated tactoid with three layers of water separating neighboring platelets.

Our results with standard topographic image and the corresponding phase signal obtained simultaneously during the same scan indicate that higher stacks of hydrated platelets have a smaller Young's modulus. This result must be a consequence of the intercalated water layers, since the Young's modulus for dry montmorillonite has been estimated to be approximately the same as that for dry mica.[24]

Our ability to measure plate heights to less than 0.02 nm with 95% confidence allows us to easily measure the nanoscale effects of swelling and to distinguish between the various hydration states observed and characterized by others. We are also now able to study the effects of changes in the chemical environment. Increasing NaCl content in solution has little effect on the inter-platelet separation distance for Na-MMT.

References

1 Mesri, G. & Olson, R. E. Consolidation characteristics of montmorillonite. *Geotechnique* **21**, 341-& (1971).

2 Fripiat, J., Cases, J., Francois, M. & Letellier, M. Thermodynamic and microdynamic behavior of water in clay suspensions and gels. *Journal of Colloid and Interface Science* **89**, 378-400 (1982).

3 Gee, M. L., McGuiggan, P. M., Israelachvili, J. N. & Homola, A. M. Liquid to solid-like transitions of molecularly thin-films under shear. *Journal of Chemical Physics* **93**, 1895-1906 (1990).

4 Antognozzi, M., Humphris, A. D. L. & Miles, M. J. Observation of molecular layering in a confined water film and study of the layers viscoelastic properties. *Applied Physics Letters* **78**, 300-302 (2001).

5 Mitchell, J. K., Soga, Ken'ichi. *Fundamentals of Soil Behavior*. 3rd edn, (John Wiley & Sons, 2005).

6 Delville, A. & Letellier, M. Structure and dynamics of simple liquids in heterogeneous condition - an NMR-study of the clay water interface. *Langmuir* **11**, 1361-1367 (1995).

7 Porion, P., Faugere, A. M. & Delville, A. Li-7 NMR spectroscopy and multiquantum relaxation as a probe of the microstructure and dynamics of confined Li^+ cations: An application to dense clay sediments. *J. Phys. Chem. C* **112**, 9808-9821 (2008).

8 Porion, P., Faugere, A. M. & Delville, A. Long-time scale ionic dynamics in dense clay sediments measured by the frequency variation of the Li-7 multiple-quantum NMR relaxation rates in relation with a multiscale modeling. *J. Phys. Chem. C* **113**, 10580-10597 (2009).

9 Porion, P., Michot, L. J., Faugere, A. M. & Delville, A. Influence of confinement on the long-range mobility of water molecules within clay aggregates: A H-2 NMR analysis using spin-locking relaxation rates. *J. Phys. Chem. C* **111**, 13117-13128 (2007).

10 Porion, P., Michot, L. J., Faugere, A. M. & Delville, A. Structural and dynamical properties of the water molecules confined in dense clay sediments: A study combining H-2 NMR spectroscopy and multiscale numerical modeling. *J. Phys. Chem. C* **111**, 5441-5453 (2007).

11 Singh, P. N. & Wallender, W. W. Effects of adsorbed water layer in predicting saturated hydraulic conductivity for clays with Kozeny-Carman equation. *J Geotech Geoenviron* **134**, 829-836 (2008).

12 Cadene, A., Durand-Vidal, S., Turq, P. & Brendle, J. Study of individual Na-montmorillonite particles size, morphology, and apparent charge. *Journal of Colloid and Interface Science* **285**, 719-730 (2005).

13 Dove, P. M. & Chermak, J. A. in *Scanning Probe Microscopy of Clay Minerals* Vol. 7 *CMS Workshop Lectures* (eds K. L. Nagy & A. E. Blum) 139-170 (The Clay Minerals Society, 1994).

14 Otsuka, I., Yaoita, M., Higano, M., Nagashima, S. & Kataoka, R. Tapping mode AFM study on the surface dynamics of a single glucose oxidase molecule on a Au(111) surface in water with implication for a surface-induced unfolding pathway. *Applied Surface Science* **235**, 188-196 (2004).

15 Mitchell, J. K. *Fundamentals of Soil Behavior*. 2 edn, (John Wiley & Sons, Inc., 1993).

16 Verdaguer, A., Sacha, G. M., Bluhm, H. & Salmeron, M. Molecular structure of water at interfaces: Wetting at the nanometer scale. *Chemical Reviews* **106**, 1478-1510 (2006).

17 Cases, J. M. *et al.* Mechanism of adsorption and desorption of water-vapor by homoionic montmorillonite. 1. The sodium-exchanged form. *Langmuir* **8**, 2730-2739 (1992).

18 Delville, A. Modeling the clay water interface. *Langmuir* **7**, 547-555 (1991).

19 Delville, A. Structure of liquids at a solid interface - an application to the swelling of clay by water. *Langmuir* **8**, 1796-1805 (1992).

20 Delville, A. Structure and properties of confined liquids - a molecular-model of the clay water interface. *Journal of Physical Chemistry* **97**, 9703-9712 (1993).

21 Delville, A. Monte-Carlo simulations of surface hydration - an application to clay wetting. *Journal of Physical Chemistry* **99**, 2033-2037 (1995).

22 Suzuki, S. & Kawamura, K. Study of vibrational spectra of interlayer water in sodium beidellite by molecular dynamics simulations. *J. Phys. Chem. B* **108**, 13468-13474 (2004).

23 Hall, P. L., Harrison, R., Hayes, M. H. B., Tuck, J. J. & Ross, D. K. Particle orientation distributions and stacking arrangements in size-fractionated montmorillonite measured by neutron and X-ray-diffraction. *Journal of the Chemical Society-Faraday Transactions I* **79**, 1687-1700 (1983).

24 Chen, B. Q. & Evans, J. R. G. Elastic moduli of clay platelets. *Scripta Materialia* **54**, 1581-1585, doi:10.1016/j.scriptamat.2006.01.018 (2006).

25 Singh, P. N. and W. W. Wallender. Effects of adsorbed water layer in predicting saturated hydraulic conductivity for clays with Kozeny-Carman equation. *Journal of Geotechnical and Geoenvironmental Engineering* **134 (6)**, 829-836 (2008)

This research was funded by the Kearney Foundation of Soil Science: Understanding and Managing Soil-Ecosystem Functions Across Spatial and Temporal Scales, 2006-2011 Mission (http://kearney.ucdavis.edu). The Kearney Foundation is an endowed research program created to encourage and support research in the fields of soil, plant nutrition, and water science within the Division of Agriculture and Natural Resources of the University of California.